An Enhanced Time-reversal Imaging Algorithm-driven Sparse Linear Array for Progressive and Quantitative Monitoring of Cracks

Qiang Wang, Yanfeng Xu, Zhongqing Su, Maosen Cao, Dong Yue

Submitted to ***IEEE Transactions on Instrumentation and Measurement*** on 31 May 2018. Revised and resubmitted on August 24, 2018. This work was supported by the China Postdoctoral Science Foundation (Grant No. 2015M570401), in part by the Institute of Advanced Technology Open Fund of Nanjing University of Posts and Telecommunications (Grant No. XJKY15005), in part by the Research Foundation of Nanjing University of Posts and Telecommunications (Grant Nos. NY215093 and NY217070). (*Corresponding author: Qiang Wang*)

Qiang Wang and Dong Yue are with School of Automation, Nanjing University of Posts and Telecommunications, Nanjing, China (e-mail: wangqiang@njupt.edu.cn).

Yanfeng Xu and Zhongqing Su are with the Department of Mechanical Engineering, The Hong Kong Polytechnic University, Kowloon, Hong Kong SAR, China.

Maosen Cao is with Department of Engineering Mechanics, Hohai University, Nanjing, China.

***Abstract* —** A Lamb wave and linear PZT array based monitoring method for the detection and quantification of crack damage is presented in this paper. Because existing PZT array arrangements are not suitable for quantitative monitoring of crack damage both in orientation and in length, a sparse linear PZT array is introduced and applied to collect crack reflections. Based on this new array, a method for estimating crack orientation is proposed. An amplitude spectrum as a function of angle is mapped using time delayed and summed signals. By finding the peaks in the spectra, the central actuator element and corresponding orientation angle are determined. Furthermore, the *ToF* imaging method is modified to display and evaluate cracks quantitatively. Validating experiments are conducted on a T6061 aluminum plate, monitoring and evaluating single and connected cracks with various orientations in different locations. As suggested by the experiments, the orientation of most cracks can be well recognized and all cracks can be quantitatively displayed by the proposed methods.

***Index Terms*—Sensor arrays; crack detection; monitoring; waveguide theory; signal processing.**

I. INTRODUCTION

Real-time detection and quantitative assessment of damage in metallic plate-like structures are of great significance for structural health monitoring. In consideration of the merits of low attenuation and high sensitivity to tiny discontinuities like cracks in a plate, Lamb wave based techniques using embedded sensor/actuator networks have attracted much attention [1-6]. Confirming the presence of damage is the basic requirement for detecting damage, achieved by comparing Lamb wave signals received from a damaged structure with those from an intact structure [7, 8]. Further detection and tracking of crack growth, including monitoring changes in both size and orientation trends, have exhibited potential value, especially for early stage cracks [9].

Crack growth is generally known to be an irregular process. Thus, a crack model cannot simply assume that damage is perpendicular to the propagation direction of Lamb wave [10]. To cope with this wave obliqueness, a common method is to build the relationship between crack length and features of measured data, such as transmission [11, 12], reflection coefficient [10], or time of flight (*ToF*) [3, 7]. For tiny cracks, shorter than wavelength, experimental results in [14] indicate that scattered signal amplitude is linearly proportional to crack size. Furthermore, some advanced algorithms, such as the Bayesian method [15] and particle filter [16,17], have been used to predict the growth trend of lengthening cracks. Published research has mainly focused on quantitative assessment of crack length; few studies have investigated crack orientation. One feasible solution is a Lamb wave based imaging method with high resolution that distinguishes the two ends of a crack as two highlighted spots in the image [18]. This work has been limited to scenarios in which the location of a crack relative to a sensor network must be known. However, real crack occurrence is irregular and location is uncertain.

With the aim of resolving this problem, a novel technique is proposed in this paper. As the phase information or arriving time delay of the crack reflection indicates the orientation of the damage, through extracting the time delays of signals received from two adjacent sensors and comparing their time delays, the orientation of the crack can be calculated.

Furthermore, to effectively collect information about the orientation of crack damage, the arrangement scheme of piezoelectric lead zirconate titanate (PZT) should be designed and imposed. Basically, PZT arrays can be divided into two types: distributed array [19-25] and centralized array [26-29]. In a distributed PZT array with large detection range, damage can be illuminated from different directions. In this arrangement, scattered wave from the damage is mainly received by sensors based on the diffuse reflection of Lamb wave, which makes less contribution than reflection to calculating orientation. In a centralized PZT array, the PZT sensor/actuators are often linearly arranged close to each other to compose a dense array. This type of array is effective for receiving reflection from a crack, but inevitably is restricted to a very small detection area. Therefore, based on a combination having the advantages of these two traditional PZT arrays, a sparse linear array is applied in this work. The interval between each element of the linear PZT array is increased to cover the entire width of a structure and to increase the area of detection.

II. Modified linear PZT array for Lamb wave based monitoring of crack damage

A. Modified linear PZT array for the collection of crack reflections

Damage monitoring methodologies based on the scattering of Lamb wave are effective for many types of damage, including common impact holes, composite delamination, corrosion, etc. However, with crack or notch damage, specular reflections rather than diffuse reflections are probably likely to dominate reception. Hence, although a traditional distributed PZT array has the advantage in large-area detection, it is limited in processing specular reflections of crack damage, so that only a few actuator-sensor pairs of the array can capture the reflection signals. A linear centralized array is more effective than a distributed array for collecting the orientation information of crack damage by extracting the arriving time delays of the received reflections. Nevertheless, with the limitation in length of a centralized array, the scanning area is always small. In this work, a linear centralized array is extended to cover the entire edge of a structure, as shown in Fig. 1. With an increased interval of the array (longer than half a wavelength), even at the expense of the quality of beam synthesis and imaging, the propagation time difference of each adjacent sensed damage reflection should be more easily distinguished, and more reflections would be received by the sensor array. Generally, the location of the array depends on its monitoring area to be concerned. Based on the far field theory, similar to phased array techniques [27-28], there should be a certain distance (normally several wavelength) between the array and its monitoring area to reduce measurement errors caused by the non-parallelism of the wave front.

B. Evaluation of orientation of crack damage using a modified linear array

Because the wavefront of a reflected signal is approximately linear in the far field, the orientation of a crack can be calculated by comparing the arriving time delays of the sensing signals of adjacent sensors. As shown in Fig. 1, the element n acts as the actuator and the adjacent element k is used to receive the reflection wave as a sensor. Under the far-field condition, the incident direction θ of the actuator element n is identical to the direction of the signal received from sensor element k. Clearly, when the incident direction coincides with the normal line of orientation of a crack, the amplitude of the sensed signal of sensor k achieves or tends to maximum [30]. At the same time, the signal processed by the time delay and sum (DAS) of signals received from all adjacent sensors also achieves maximum. If the actuator n is assumed as reference point, the time delay of sensor k can be written as

$$\Delta t_{kn} = ds_{kn}/v = (k-n)l\cos\theta/v \quad (1)$$

where v is the velocity of the excited Lamb wave mode, ds_{kn} is the difference in distance of the Lamb wave between the sensor k and the actuator n in the propagation direction, and l is the interval between adjacent elements. Because the initial crack damage is usually very short, the width of the reflected beam is also short and only a few elements around the actuator are required. To reduce data redundancy and improve calculation efficiency, therefore, a moving window with $2p+1$ (p=1, 2, 3, …) elements are considered. Through scanning the actuator n and searching the angle θ, the central actuator number n_c and the angle θ_c that correspond to the normal direction of the crack can be obtained because the DAS signal is maximal. This orientation detection process can be expressed as

$$[n_c, \theta_c] = \max\left[\left|\sum_{k=n-p}^{n+p} f_{kn}(t - \Delta t_{kn})\right|_{n,\theta}\right] \tag{2}$$

where f_{kn} is the damage scattered signal actuated by element n and sensed by element k, $n=p+1$, $p+2$, $p+3$, …, $N-p$. N is the sum of the elements in the linear array.

It should be noted that in Eq. (2), there will be several local maxima if multiple crack damage exist in the structure. Thus, it is possible to detect multiple damages simultaneously. Eq. (2) then is rewritten as

$$\begin{bmatrix}\mathbf{n_c}\\ \boldsymbol{\theta}_\mathbf{c}\end{bmatrix} = \max\left[\left|\sum_{k=n-p}^{n+p} f_{nk}(t - \Delta t_{kn})\right|_{n,\theta}\right], \mathbf{n_c} = [n_{c1}, n_{c2}, n_{c3}, \cdots], \boldsymbol{\theta}_\mathbf{c} = [\theta_{c1}, \theta_{c2}, \theta_{c3}, \cdots] \tag{3}$$

Here, each pair $[n_{cm}, \theta_{cm}]$ represents one possible crack and m=1, 2, 3, …. In general, it is complex to determine orientation when the location is unknown. But this method can obtain the orientation without a priori knowledge. It should be noted that due to the limited number of elements and the sensing signals in single array, the more the damage is, the more complex the reflection is. Thus, when much more damages happen, the pseudo local maxima may be increased in the DAS signal which decreased the accuracy of monitoring, and the damage shadowed by others is probably hard to be found because of no scattering signal, especially the small one. One more array can be added in other direction to compensate for this problem.

C. Crack damage imaging and evaluation

As discussed above, detection of orientation of crack damage can be achieved by calculating the synchronization of the reflected signals captured by the array. Therefore, *ToF* is the selected characteristic parameter. At the same time, the imaging method based on *ToF* is effective in searching for possible multiple damage in a structure using a limited number of sensors [31-34]. The *ToF*-based imaging algorithm is applied with the field value S at pixel (x, y), defined as

$$\begin{cases} S(x,y)=\sum_{k=1}^{N} A_{nk}\, f_{nk}\left(t_0+\dfrac{R_{xy}^{n}+R_{xy}^{k}}{v}\right) \\ R_{xy}^{n}=\sqrt{(x-x_n)^2+(y-y_n)^2},\quad R_{xy}^{k}=\sqrt{(x-x_k)^2+(y-y_k)^2} \end{cases} \tag{4}$$

where A_{kn} is the compensation coefficient for different attenuation and possible performance differences, t_0 is the starting time of the Lamb wave excitation, R_{xy}^{n} and R_{xy}^{k} are the distances from pixel (x, y) to the element n and k respectively. This method is adopted here and further improved for crack detection and evaluation. Two concerns are addressed in the research: a) The boundary reflection of the plate is similar to the reflection from the crack and thus may create artefacts in the imaging; b) How to express the length of a detected crack. With the traditional imaging method, the damage region is searched and highlighted by the intersection of many elliptical images, in most cases causing the final image to exceed the scope of the damage area.

In the imaging process, all the received signals are delayed according to the orientation of the crack that is first detected. Though this post-processing, the direction of the array is virtually rotated with sensor *n* as the center to be parallel to the crack, as shown in Fig. 2. Then the arrival times and phases of all the crack reflections become consistent. These reflected signals are superimposed and enhanced during imaging. On the other hand, if the crack is not parallel to the plate boundary, the boundary reflection cannot become consistent and is counteracted in the imaging. For each imaging ellipse and actuator-sensor pair, the possible location of the crack should be around the intersection of the ellipse and the perpendicular bisector of the actuator-sensor pair. Thus, only the points around the intersection need to be assigned during imaging. For any possible crack and identified [n_{cm}, θ_{cm}], the modified assignation process for image pixel (x, y) can be expressed as:

$$\begin{cases} S_m(x,y) = \sum_{k=1}^{N} A_{nk} f_{nk}\left(t_0 + \dfrac{R_{xy}^n + R_{xy}^k}{v}\right) e^{\frac{-r}{\sigma}} \Big|_{n=n_{cm}} \\ R_{xy}^n = \sqrt{(x-x_n)^2 + (y-y_n)^2} \\ R_{xy}^k = \sqrt{(x - x_k + ds_{kn}\cos\theta_{cm})^2 + (y - y_k + ds_{kn}\sin\theta_{cm})^2} \end{cases} \tag{5}$$

where r is the distance from (x, y) to the intersection of the imaging ellipse and the perpendicular bisector of the actuator-sensor pair, σ is the attenuation coefficient.

III. EXPERIMENTAL RESEARCH

Two experiments were performed to validate the crack evaluation and imaging method. The first illustrated the ability to detect and evaluate the feature of orientation in two typical scenarios, including one single and two connected cracks. The monitoring results were also shown by imaging. The second experiment demonstrated that the method monitored and tracked crack growth from the initial occurrence and progress through several statuses, a very important condition to ensure structural safety.

A. Experimental setup

An aluminum plate (6061-T6, density: 2711 kg/m^3, and Young's modulus: 71 GPa) with the dimensions 600 mm × 600 mm × 2 mm was used, as shown in Fig. 3. A linear PZT array composed of 15 PZT elements (1#~15#) was located about 100 mm from the plate boundary. The type of the PZT element is PSN-33. Its piezoelectric constant d_{31} is 160×10^{-12} C/N and resonant frequency is around 200 kHz. All PZT elements are 8 mm in diameter and 0.48 mm in thickness. The interval between adjacent PZT elements in the array was 30 mm. The cracks and their growth were simulated by attaching metal bars and cutting grooves. Thus cracks in different directions and locations were artificially produced.

An integrated Lamb wave modularized structural health diagnosis system was used to generate and collect the Lamb wave structural responses [34]. Studies have shown that the mode selection can be achieved by tuning the frequency of narrow band excitation to obtain a single mode mainly Lamb wave signal, for example, S0 or A0 [20]. Damage detection capability, signal conditioning difficulty and PZT actuator working efficiency are also taken into account in the experimental research. An NI® PXI-5412 arbitrary waveform generator (AWG) with a sampling rate of up to 100 MS/s was utilized to excite S0 Lamb wave mode with Hanning window-modulated five-cycle sinusoidal tone bursts at the central frequency of 200 kHz. Lamb wave signals were observed using an 8-channel NI® PXI-5105 oscilloscope module with a sampling rate of up to 60 MHz per channel. An NI® PXI-2529 high-density matrix switch was used to control selection of the actuator-sensor pairs. An APA40 linear power amplifier and an EO-LNa-3 pre-amplifier were also used in the measurement system. All the modules were integrated on a PXI bus platform (NI® PXIe-1071) to configure a compact diagnosis system.

B. Experimental results

1) Evaluation of crack orientation

To verify the orientation evaluation method, two kinds of artificial damage were studied in this experiment: (a) a single 100 m crack with normal direction 60° and (b) two connected cracks (like hole-edge cracks) with lengths of 100 mm and 145 mm and normal directions of 135° and 60° respectively, as shown in Fig. 4.

(a) Single crack

The waveform of five-cycle tone bursts shown in Fig. 5(a) was output from the AWG to actuate element 9#. Baseline Lamb wave signals of the array in a plate without damage are shown in Fig. 5(b). The sensed wave contains the crosstalk wave induced by the electric circuit, direct waves from the actuator (element 9# in this figure) to other sensors, and boundary reflections. When the single artificial crack C1 100 mm in length was located at the right of the center of the plate, as shown in Fig. 4(a), the damage reflections were obtained by comparing the baseline signal and received signal in the damaged structure, as shown in Fig. 5(c). As well as the unwanted direct waves and boundary reflections, crosstalk waves existing in all element sensors were eliminated. The first arriving wave packet was the reflected S0 wave mode from the crack C1. Other later arriving wave packets in the array signals were composed of mode conversion and multiple reflections, but only the first arriving wave packet was useful for the orientation evaluation. For each actuator, as the tuning angle changed, the temporal and angular spectrum was mapped by a set of DAS signals according to Eqs. (2) and (3), as depicted in Fig. 6. The scanning angle θ tuned from 35° to 145° and the number of elements in the moving window (shown in Fig. 1) was set at five (p=2) in the monitoring. Then the orientation (normal direction of the crack) equaled the tuning angle corresponding to the maximum amplitude of the spectrum. In this spectrum, when the tuned angle was around 62°, the spectrum amplitude reached the maximum. As the window was moved, elements 3# to 13# sequentially acted as actuator, and several spectra were obtained, as shown in Fig. 6. From these spectra, it can be read that the maximum appearing as the center element n_{c1} is 9# and the angle θ_{c1} is 62°. Therefore, it could be seen that when the actuator was located on the normal line of the crack, the amplitude of the processed signal achieved its maximum.

In accordance with the evaluated crack features of center n_c and orientation θ_c, the damage imaging could be reconstructed using the assigning equation given as Eq. (5). The imaging result for the crack C1 in Fig. 4(a) is shown in Fig. 7(a). Thresholding was employed, and the value was set at half of the maximum pixel value of the images. This same thresholding value was adopted for the other images in this paper. From the imaging result, cracks are revealed and their orientation and length can be determined from the monitoring result, that is identical to the practice crack marked in red. There is almost no interference from boundary reflections. The artefacts parallel to the crack image are caused by the re-reflection of the boundary below the linear array and can be further eliminated by thresholding.

For comparison, the measured array data was used to reconstruct the damage imaging by the traditional *ToF* damage imaging method, as shown in Fig. 7(b). For single crack damage, both methods can obviously reveal the damage region. The difference is that the *ToF* damage imaging suffers severe influence from the boundary reflection. These artefacts were difficult to eliminate, although the same threshold value was used as in the modified method. At the same time, more artefacts were generated in this image, making damage estimation difficult to achieve.

(b) Two connected cracks

Cracks usually grow irregularly in all directions and can form a hole-edge crack, like the two connected cracks C2 and C3 shown in Fig. 4(b). Because the two cracks are connected, multiple reflections can be generated between them. Damage monitoring thus becomes much more complex than in single crack situations. Typically, the damage reflections actuated by element 6# and 9# are shown in Fig. 8. It can be seen clearly from figures that the incident angle of Lamb waves are different because of the different relative position between the excited elements and the normal lines of the cracks. Therefore, the reflections of the cracks C2 and C3 captured by the array are completely different. In detection of the orientation of cracks C2 and C3, Fig. 9 shows that two peaks exist in the amplitude spectra of the phase tuning and superimposing of crack reflections in accordance with Eq. (4). One peak locates at θ_{c2} of 62° excited by element 6# and the other locates at θ_{c3} of 133° excited by element 12#.

The results of use of the modified imaging and traditional *ToF* imaging methods for cracks C2 and C3 are shown in Fig. 10. The location, length, and orientation of the two connected cracks can be seen in Fig. 10(a), in which the imaging is identical to the actual damage. The figure also shows that the image of the connection of the two cracks has the highest intensity. Compared with the imaging of a single crack, the imaging quality is not decreased, but more artefacts are generated due to the multiple reflections. In the image using the traditional method (Fig. 10(b)), the cracks can scarcely be distinguished, with a low contrast ratio and high noise disturbance. Around the image of the cracks there are many artefactual regions with high intensity formed by the repeated superposition of crack reflections. Therefore, in a complex damage environment, the modified imaging method has the ability to reconstruct a higher quality image.

It is also to be concerned that for real engineering applications, the effects of ambient temperature and stress changes on the structural response signals also needs to be considered for the baseline based damage monitoring method, which will bring errors to the monitoring results. In terms of temperature compensation, there have been some achievements which were proved to be effective, such as optimal baseline selection (OBS), baseline signals stretch (BSS) or combination of OBS and BSS [35, 36].

2) Evaluation of crack growth

Crack growth from the initial appearance can be rapid; thus, quantitative monitoring and tracking is very important to ensure structural safety. A simple process of crack growth with eight statuses was observed. Fig. 11 shows that the initial length of the single crack C4 is 20 mm (*Status1*). The length gradually increases to 50 mm (*Status2*), 80 mm (*Status3*), and 100 mm (*Status4*). The normal direction of crack C4 is about 135°. Then another crack C5 is generated by cutting grooves at the end of crack C4 with the initial length of 20mm (*Status5),* with subsequent growth to 50mm (*Status6*), 80mm (*Status7*), and 110mm (*Status8*).

The entire process was monitored and tracked by the proposed method. The detected orientations of cracks C4 and C5 are listed in Table. 1. For the first four statuses, when only a single crack exists in the structure, the monitoring results of crack C4 are in good agreement with the actual situations. However, for crack C5 in the initial *Status5* and the following S*tatus6*, errors in the detected orientations are close to 20°. The reason is that the reflected signal is rather weak and is overlapped in multiple reflections, when the crack length is short. As the crack continues to grow, the primary reflection from C5 is eventually greater than other multiple reflections. Thus, errors in the detection results are greatly reduced and are only 3° and 0° respectively for *Status7* and *Status8*.

All eight statuses were then imaged based on the parameters $\boldsymbol{\theta}_c$ and $\boldsymbol{n}_c$ in Table 1, and the results are shown in Fig. 12. As in the orientation monitoring results, the monitoring results of the cracks in the first four statuses in Fig. 12(a)~(d) show good agreement with the actual situations. The only issue that needs to be noted is that the pixel values in the detected damage region in *Status1* are weak due to the short crack length and limited reflection. Fortunately, it is sufficient to show the location and orientation of the crack. The maximum deviations are still evident in the monitoring results of *Status5* and *Status6*, as shown in Fig. 12(e)~(f). For the detected $\boldsymbol{\theta}_c$ and $\boldsymbol{n}_c$ with large errors, the damage regions in the imaging of crack C5 are a little further from the actual location. This is because that the crack C5 in these two *Statuses* is relative small so that its reflection is disturbed by noises such as boundary reflection. With the subsequent growth of crack C5, the monitoring results for *Status7* and *Status8* have relatively high accuracy when compared with the actual locations, as shown in Fig. 12(g)~(h). The results of use of the traditional *ToF* imaging methods for cracks C4 and C5 are shown in Fig. 13. Similar to the comparison shown in Fig. 10, in the images using the traditional method, only the probable location of the cracks can be indicated. However, it's hard to distinguish the growing of the cracks from the images.

Compared with the existing baseline based damage detection techniques, such as the damage index based monitoring methods [37-39], the characteristic of the crack reflection field is analyzed and used in this proposed method. Therefore, the applicability of this method is more focused on crack or notch. Actually, the improvement in this paper is to detect the reflection signal wavefronts of possible cracks (also used to detect the orientation of crack) and to image them. If the reflection field is not existed, the happened damage can also be diagnosed by using the *ToF*-based imaging algorithm.

IV. Concluding Remarks

Lamb wave based quantitative crack monitoring and imaging method is the focus of this paper. A modified sparse linear PZT array was studied for capture of the reflection from the cracks to ensure the collection of sufficient damage information. Then the orientation detection algorithm and the modified *ToF* imaging method were proposed for crack monitoring based on a modified sparse linear PZT array. Several verification experiments were performed on an aluminum plate. Evaluation of $\boldsymbol{\theta}_c$ and $\boldsymbol{n}_c$ of a single crack and two connected cracks indicated that the proposed method was effective in quantitative monitoring. Using these $\boldsymbol{\theta}_c$ and $\boldsymbol{n}_c$, the images were reconstructed and the results showed improvement of the modified method compared with the traditional method. For tracking the growth of cracks connected to other cracks or featuring a change in the direction of growth, the new method showed good agreement with the actual damage growth in different statuses. When the length of one of the cracks was short, the monitoring accuracy was affected by the near crack, although the new crack could be sensed in the detection and imaging of orientation. With extension of the crack, the monitoring became more accurate and the cracks were evaluated with errors within 3°. Future research will focus on precise monitoring and evaluation of cracks in all stages.

References

1. S. Legendre, D. Massicotte, J. Goyette, T. K. Bose, “Wavelet-transform-based method of analysis for Lamb-wave ultrasonic NDE signals”, *IEEE Trans. Instrum. Meas.*, vol. 49, no. 3, pp. 524-530, Jun. 2000.
2. E. Baravelli, M. Senesi, M. Ruzzene, L. De Marchi, “Fabrication and characaterization of a wavenumber-spiral frequency-steerable acoustic transducer for source localization in plate structures”, *IEEE Trans. Instrum. Meas.*, vol. 62, no. 8, pp. 2197-2204, Aug. 2013.
3. Z. Su, L. Ye, Y. Lu, “Guided Lamb waves for identification of damage in composite structures: A review”, *J. Sound Vib.*, vol. 295, no. 3, pp. 753–780, Aug. 2006.
4. J. R. Lee, H. Tsuda, "Monitoring of cracks at an open hole using built-in fibre wave piezoelectric transducers", *Meas. Sci. Technol.*, vol.17, no. 10, pp. 2643-2649, Oct. 2006.
5. X. Zhu, P. Rizzo, A. Marzani, J. Bruck, "Ultrasonic guided waves for nondestructive evaluation/structural health monitoring of trusses", *Meas. Sci. Technol.*, vol.21, no. 4, p.045701, Apr. 2010.
6. W. J. Staszewski, B. C. Lee, R. Traynor, R, "Fatigue crack detection in metallic structures with Lamb waves and 3D laser vibrometry", *Meas. Sci. Technol.*, vol.18, no. 3, pp. 727-739, Mar. 2007.
7. A. Stawiarski, M. Barski, P. Pająk, “Fatigue crack detection and identification by the elastic wave propagation method”, *Mech. Syst. Signal Pr.*, vol. 89, no. 15, pp.

119-130, May 2017.

8. Y. K. An, J.H. Kim, H.J. Yim, "Lamb wave line sensing for crack detection in a welded stiffener", *Sensors*, vol. 14, no. 7, pp. 12871-12884, Jul. 2014.

9. B. Masserey, P. Fromme, "In-situ monitoring of fatigue crack growth using high frequency guided waves", *NDT & E Int.*, vol. 71, pp. 1-7, Apr. 2015.

10. Y. Lu, L. Ye, Z. Su, C. Yang, “Quantitative assessment of through-thickness crack size based on Lamb wave scattering in aluminium plates”, *NDT & E Int.*, vol. 41, no. 1, pp. 59-68, Jan. 2008.

11. H. Cho, C. J. Lissenden, “Structural health monitoring of fatigue crack growth in plate structures with ultrasonic guided waves”, *Struct. Health Monit.*, vol. 11, no. 4, pp. 393–404, Jul. 2012.

12. J. K. Agrahari, S. Kapuria, “Active detection of block mass and notch-type damages in metallic plates using a refined time-reversed Lamb wave technique”, *Struct. Control Health Monit.*, vol. 25, no. 2, pp. 1-18, Feb. 2018.

13. P. A. Vanniamparambil, I. Bartoli, K. Hazeli, J. Cuadra, E. Schwartz, R. Saralaya, A. Kontsos, “An integrated structural health monitoring approach for crack growth monitoring”, *J. Intel. Mat. Syst. Str.*, vol. 23, no. 14, pp. 1563–1573, Sept. 2012.

14. J. An, R. T. Haftka, N. H. Kim, F. Yuan, B. M. Kwak, H. Sohn, C. M. Yeum, “Experimental study on identifying cracks of increasing size using ultrasonic excitation”, *Struct. Health Monit.*, vol. 11, no. 1, pp. 95–108, Jan. 2012.

15. J. He, Y. Ran, B. Liu, J. Yang, X. Guan, "A Fatigue Crack Size Evaluation

Method Based on Lamb Wave Simulation and Limited Experimental Data", *Sensors*, vol. 17, no. 9, p.2097, Sep. 2017.

16. S. Yuan, J. Chen, W. Yang, L. Qiu, “On-line crack prognosis in attachment lug using Lamb wave-deterministic resampling particle filter-based method”, *Smart Mater. Struct.*, vol. 26, no. 8, p. 085016, Aug. 2017.
17. J. Chen, S. Yuan, L. Qiu, J. Cai, W. Yang, “Research on a Lamb Wave and Particle Filter-Based On-Line Crack Propagation Prognosis Method”, *Sensors*, vol. 16, no. 3, pp. 320, Mar. 2016.
18. L. Yu, C. A. Leckey, “Lamb wave–based quantitative crack detection using a focusing array algorithm”, *J. Intel. Mat. Syst. Str.*, vol. 24, no. 9, pp. 1138–1152, Jun. 2012.
19. M. Demetgul, V. Y. Senyurek, R. Uyandik, I. N. Tansel, O. Yazicioglu, "Evaluation of the health of riveted joints with active and passive structural health monitoring techniques", *Measurement*, vol. 69, pp. 42-51, Jun. 2015.
20. L. Yu, V. Giurgiutiu, “Piezoelectric Wafer Active Sensors in Lamb Wave-Based Structural Health Monitoring”, *JOM*, vol. 64, no. 7, pp. 814-822, Jul. 2012.
21. L. Qiu, S. Yuan, “On development of a multi-channel PZT array scanning system and its evaluating application on UAV wing box”, *Sensor. Actuat. A-Phys.*, vol. 151, no. 2, pp. 220-230, Apr. 2009.
22. F. Yan, J. L. Rose, R. L. Royer, “Ultrasonic Guided Wave Imaging Techniques in Structural Health Monitoring”, *J. Intel. Mat. Syst. Str.*, vol. 21, no. 3, pp. 377-384, Feb. 2010.

23. Z. Su, X. Wang, L. Cheng, L. Yu, Z. Chen, “On Selection of Data Fusion Schemes for Structural Damage Evaluation”, *Struct. Health Monit.*, vol. 8, no. 6, pp. 223-241, May 2009.

24. Q. Wang, S. Yuan, “Baseline-free Imaging Method based on New PZT Sensor Arrangements”, *J. Intel. Mat. Syst. Str.*, vol. 20, no. 14, pp. 1663-1673, Sept. 2009.

25. X. Chen, J. E. Michaels, T. E. Michaels, “A Methodology for Estimating Guided Wave Scattering Patterns From Sparse Transducer Array Measurements”, *IEEE Trans. Ultrason. Ferroelectr. Freq. Control*, vol. 62, no. 1, pp. 208-219, Jan. 2015

26. F. Li, H. Peng, G. Meng, G,"Quantitative damage image construction in plate structures using a circular PZT array and lamb waves", *Sensor. Actuat. A-Phys.*, vol. 214, no. 4, pp. 66-73, Aug. 2014.

27. L. Yu, V. Giurgiutiu, “In-situ optimized PWAS phased arrays for Lamb wave structural health monitoring”, *J. Mech. Mater. Struct.*, vol. 2, no. 3, pp. 459-487, May 2007.

28. W. Liu, J. W. Hong, “Three-dimensional Lamb wave propagation excited by a phased piezoelectric array”, *Smart Mater. Struct.*, vol. 19, no. 8, p. 085002, Jun. 2010.

29. G. Aranguren, P. M. Monje, V. Cokonaj, E. Barrera, M. Ruiz, "Ultrasonic wave-based structural health monitoring embedded instrument", *Rev. Sci. Instrum.*, vol. 84, no. 12, p. 125106, Dec. 2013.

30. P. Fromme, “Lamb wave (A0 mode) scattering directionality at defects”, in *Proc.*

43rd QNDE, Atlanta, GA, USA, pp. 030002-1-030002-9, Jul. 2016.

31. F. Li, Z. Su, L .Ye, G. Meng, "A correlation filtering-based matching pursuit (CF-MP) for damage identification using Lamb waves", *Smart Mater. Struct.*, vol. 15, no. 6, pp. 1585-1594, Oct. 2006.
32. P. Blanloeuil, L. R. F. Rose, J. A. Guinto, M. Veidt, C. H. Wang, "Closed crack imaging using time reversal method based on fundamental and second harmonic scattering", *Wave Motion*, vol. 66, no. 1, pp. 156-176, Nov. 2016.
33. L. Zeng, M. Zhao, J. Lin, W. Wu, "Waveform separation and image fusion for Lamb waves inspection resolution improvement", *NDT & E Int.*, vol. 79, no. 1, pp. 17-29, Apr. 2016.
34. Q. Wang, M. Hong, Z. Su, "An In-Situ Structural Health Diagnosis Technique and Its Realization via a Modularized System", *IEEE T. Intrum. Meas.*, vol. 64, no. 4, pp. 873-887, Apr. 2015.
35. A. J. Croxford, J. Moll, P. D. Wilcox, J. E. Michaels, "Efficient temperature compensation strategies for guided wave structural health monitoring", *Ultrasonics*, vol. 50, no. 4, pp. 517-528, Apr. 2010.
36. T. Clarke, P. Cawley, P. D. Wilcox, and A. J. Croxford, "Evaluation of the damage detection capability of a sparse-array guided-wave SHM system applied to a complex structure under varying thermal conditions," *IEEE Trans. Ultrason. Ferroelectr. Freq. Control*, vol. 56, pp. 2666-2678, Dec. 2009.
37. N. Chakraborty, V.T. Rathod, D. Roy Mahapatra, S. Gopalakrishnan, "Guided wave based detection of damage in honeycomb core sandwich structures", *NDT*

& E Int., vol. 49, pp.27-33, Jul. 2012.

38. V.T. Rathod, D. Roy Mahapatra, "Ultrasonic Lamb wave based monitoring of corrosion type of damage in plate using a circular array of piezoelectric transducers", *NDT & E Int.*, vol. 44, pp. 628-636, Nov. 2011.
39. G. Giridhara, V.T. Rathod, S. Naik, D. Roy Mahapatra, S. Gopalakrishnan, "Rapid localization of damage using a circular sensor array and Lamb wave based triangulation", *Mech. Syst. Signal Pr.*, vol.24, no. 8, pp. 2929-2946, Nov. 2010.

Qiang Wang received his B.Sc. from Yanshan University, Qinhuangdao, China in 2002, and M.Eng. and Ph.D. degrees from Naijing University of Aeronautics and Astronautics, Nanjing, China in 2005 and 2009, respectively. He is an Associate Professor with the School of Automation, Nanjing University of Posts and Telecommunications, Nanjing, China. From 2011 to 2012, he was a Research Associate with the Department of Mechanical Engineering, The Hong Kong Polytechnic University. He has published over 10 refereed international journal papers and 10 conference papers. His research interests include structural health monitoring, smart materials and structures, sensors, and digital signal processing.

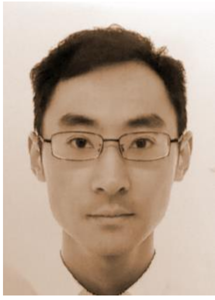

Yanfeng Xu was born in Shanghai, China, in 1988. He received B.S. degree in applied physics and acoustics from Tongji University, China, in 2011. He received Ph. D. degree in acoustics from the Institute of Acoustics at Tongji University, in 2017. He currently is postdoctoral research fellow with Department of mechanical Engineering, Hong Kong Polytechnic University. His research interests mainly focus on NDT, including laser ultrasonics, ultrasonic imaging, guided wave inspection and signal processing.

Zhongqing Su received his B.Sc. and M.S. degrees from Beijing University of Aeronautics and Astronautics, China in 1997 and 2000, respectively, and Ph.D. degree in 2004 from the School of Aerospace, Mechanical and Mechatronic Engineering at the University of Sydney, Australia. He is now a Professor affiliated with the Department of Mechanical Engineering at the Hong Kong Polytechnic University, Hong Kong. He is the author/co-author of two monographs, four edited books and international conference proceedings, six book chapters, and over 130 refereed international journal papers and 100 international conference papers. He was awarded the Structural Health Monitoring – Person of the Year (SHM-POY) in 2012. He been an Associate Editor for Ultrasonics, a Subject Editor for Journal of Sound and Vibration, an Associate Editor for Structural Health Monitoring: An International Journal, and an Associate Editor for ASME Journal of Nondestructive Evaluation, Diagnostics and Prognostics of Engineering Systems. He is also the Chairman of the 7th Asia-Pacific Workshop on Structural Health Monitoring (APWSHM-2018), to be held in 2018 in Hong Kong.

Maosen Cao received his PhD in 2005 from the College of Civil Engineering at Hohai University, also winning the National Doctoral Dissertation Award. He is a full professor in the Department of Engineering Mechanics at Hohai University, PRC. His specific areas of interest relate to structural durability and integrity assessment, health monitoring, damage modeling and identification, disaster prevention and mitigation, and multiscale vibration and dynamics. He conducted research into structural vibration and health monitoring for six years at Washington State University, the Hong Kong Polytechnic University, and the Polish Academy of Sciences (PAS). During 2012 through 2013, he conducted collaborative research with Prof. W. Ostachowicz in PAS, supported by the Marie Curie Fellowship for experienced researchers funded by the European Commission. He is the author/co-author of 150 papers in structural vibration analysis, health monitoring, and integrity assessment, including over 50 papers in top-tier international journals such as SHM, JSV, MSSP, SMS, IJSS, and APL, with high IF and citations (600+ in Web of Science). He was awarded the prestigious European-Chinese Dragon-STAR Innovation Award, funded by the European Commission; two National Natural Science Awards of MOE in PRC. Dr Cao has contributed to a number of international conferences. He was the Chair of the 19th International Conference on Vibration Theories, Approaches and Technologies in Infrastructure Engineering, the Vice-Chair of Organization Committee of the 3rd International Conference on Structural Health Monitoring and Integrity Management, and the Technical Committee Chair of the 3rd Annual Conference of Mechanics and Mechanical Engineering. He has delivered over 40 plenary speeches, invited talks, and public seminars at international conferences and universities in various countries. He is currently a member of the Editorial Board of the Journal of Vibroengineering, Vibroengineering Procedia, and the Journal of Measurement in Engineering, and was the Guest Editor of Complexity, Shock and Vibration.

Dong Yue received the Ph.D. degree from the South China University of Technology, Guangzhou, China, in 1995. He is currently a professor and dean of the Institute of Advanced Technology and College of Automation, Nanjing University of Posts and Telecommunications and also a Changjiang Professor with the Department of Control Science and Engineering, Huazhong University of Science and Technology. He is currently an Associate Editor of the IEEE Control Systems Society Conference Editorial Board and also an Associate Editor of the IEEE Transactions on Neural Networks and Learning Systems, the Journal of the Franklin Institute and the International Journal of Systems Science. Up to now, he has published more than 100 papers in international journals. His research interests include analysis and synthesis of networked control systems, multi-agent systems, optimal control of power systems, and internet of things.